Journal of Materials Chemistry C

RSC Publishing

PAPER

View Article Online
View Journal | View Issue

Towards the limit of ferroelectric nanostructures: switchable sub-10 nm nanoisland arrays†

Cite this: *J. Mater. Chem. C*, 2013, **1**, 5299

Youngsuk Kim,‡[a] Yunseok Kim,*[bc] Hee Han,[d] Stephen Jesse,[b] Seung Hyun,[a] Woo Lee,[d] Sergei V. Kalinin[b] and Jin Kon Kim*[a]

Received 24th May 2013
Accepted 4th July 2013

DOI: 10.1039/c3tc30971a

www.rsc.org/MaterialsC

Ultrahigh density arrays of ferroelectric $PbTiO_3$ (PTO) nanoislands with various feature sizes were epitaxially grown by utilizing block copolymer micelles. Piezoresponse and ferroelectric properties were clearly observed in the PTO nanoislands by band excitation piezoresponse force microscopy. In particular, PTO nanoislands were fully switchable even with a volume as small as 79 nm^3. Accordingly, it is expected that the volume of the switchable ferroelectric nanoislands can be further decreased. The obtained results show that an areal density of over 10 Tb in^{-2} for the ferroelectric memory devices would be possible.

Introduction

Ferroelectrics have spontaneous polarization, the directions of which can be manipulated by an external electric field. This basic nature of ferroelectrics allows ferroelectric materials to be employed as nonvolatile data storage media.[1,2] With the increasing demand for miniaturization of electronic devices, ferroelectric nanostructures have attracted great interest.[3–5] However, one of the most critical issues is fabrication of ferroelectric nanostructures with switchable polarization states because ferroelectricity disappears below a certain physical dimension, *i.e.* a critical size. While ferroelectric thin films with thickness of a few unit cells are able to maintain spontaneous polarization,[6] spontaneous polarization would become unstable for discrete ferroelectric nanostructures with sizes below 10 nm due to additional free surfaces and higher depolarizing fields. Even though various approaches for fabricating ferroelectric nanostructures have been developed to improve ferroelectricity,[4,7–11] realization of ferroelectric nanostructures with feature sizes of sub-10 nm still remains a great challenge. While some research groups[12–14] recently employed ferroelectric powders with a diameter of ~10 nm to investigate the size effect on ferroelectricity, the measured ferroelectricity represented collective properties of randomly oriented powders, which can be different from those of individual ones. Thus, to study ferroelectric properties of individual nanostructures, the structure should be prepared so as to be isolated from each other and have identical physical dimensions and crystallographic orientation. We previously reported that although individual disk-shaped $PbTiO_3$ (PTO) nanoislands with an average volume (V_{NI}) of 2660 nm^3 (a diameter of 22 nm and a thickness of 7 nm) exhibit distinctive spontaneous polarization,[15] switchability of the polarization was not achieved. In this study, we downsized V_{NI} to as small as 79 nm^3 (a diameter of 7.5 nm and a thickness of 1.8 nm) by utilizing block copolymer self-assembly, and observed hysteresis loops from individual nanoislands, which suggests that nanoislands of the sub-10 nm regime are fully functional ferroelectrics and ferroelectric critical size could be further downsized.

Experiment

Polystyrene-*block*-poly(4-vinylpyridine) copolymer (PS-*b*-P4VP) was purchased from Polymer Source Inc. The molecular weights of PS and P4VP blocks are 21 000 and 4000, respectively. PS-*b*-P4VP was dissolved in PTO precursor solution (0.4 M in 2-methoxyethanol, 10% excess Pb, INOSTEK Inc.). The precursor solution was further diluted with 2-methoxyethanol (Sigma-Aldrich) to have three different concentrations (0.03, 0.02, and 0.01 M). Because the concentration of PS-*b*-P4VP in three different precursor solutions was fixed as 1.5 wt%, the molar ratios of the precursor to pyridine in three solutions are 1.33, 0.875, and 0.438, as shown in Table 1. In this situation, the PS block became the core and the P4VP block became the corona. Then, toluene, a highly selective solvent for PS, was added to induce inversion between the core and the corona; thus the P4VP block including the PTO precursor became the core of the micelles.[16–21] Toluene was chosen to stabilize precursor-loaded

[a]*National Creative Research Initiative Center for Block Copolymer Self-Assembly and Department of Chemical Engineering, Pohang University of Science and Technology (POSTECH), Pohang, Kyungbuk 790-784, Korea. E-mail: jkkim@postech.ac.kr*

[b]*The Center for Nanophase Materials Sciences, Oak Ridge National Laboratory, Oak Ridge, TN 37831, USA*

[c]*School of Advanced Materials Science and Engineering, Sungkyunkwan University, Suwon, Gyeonggi-do 440-746, Republic of Korea. E-mail: yunseokkim@skku.edu*

[d]*Korea Research Institute of Standards and Science (KRISS), Yuseong, Daejeon 305-340, Korea*

† Electronic supplementary information (ESI) available. See DOI: 10.1039/c3tc30971a

‡ Present address: LG Chem Research Park, 188, Moonji-ro, Yuseong-gu, Daejeon 305-738, Korea.

Table 1 Structural parameters of the PTO nanoisland arrays

Sample ID	[Precursor]/[pyridine]	d_{NI} (nm)	h_{NI} (nm)	Scaling ratio (d_{NI}/h_{NI})	V_{NI} (nm^3)
A	1.33	14.0 ± 4.7	5.0 ± 1.0	2.8	770
B	0.875	10.4 ± 3.2	4.1 ± 0.9	2.5	348
C	0.438	7.5 ± 2.7	1.8 ± 0.6	4.2	79

micelles, in which exchange of PS-*b*-P4VP single chains, called 'unimers', between micelles is highly improbable. The portion of surface area per single chain became large upon decreasing size due to lower aggregation number of smaller micelles. If the solvents do not have sufficient selectivity, for instance tetrahydrofuran (THF) or THF–toluene mixture, the precursor can be exposed to the solvents during unimer exchange and precipitation of the precursor can be invoked. Monolayers of spherical micelles were formed by spin-coating at a rotating speed of 2000 rpm. Single-crystalline Nb-doped $SrTiO_3$(100) (STO:Nb, Crystek) was used as a substrate. The surface of the substrates was treated with a buffered oxide etchant (JT Bakers) and thermally reconstructed.[15] The block copolymers were removed by thermal treatment at 300 °C for 15 min, and the organic moieties of the PTO precursor were completely removed by subsequent treatment at 500 °C for 15 min in an air environment. During the process, the PTO precursor became epitaxially crystallized into PTO nanoislands on the substrate. We used the PTO precursor with a molar ratio of Pb to Ti of 1.1 due to the volatility of Pb during high temperature thermal treatment.

Surface morphology of the PTO nanoislands was observed by scanning electron microscopy (SEM, Hitachi, S4800) and atomic force microscopy (AFM, Digital Instrument) with tapping mode. The crystal structure of PTO nanoislands was characterized by synchrotron X-ray diffraction (XRD, Pohang Accelerator Laboratory, 3C2 and 10C1 beamlines). High-resolution transmission electron microscopy (HRTEM, JEOL, JEM-2100F) was used to observe the cross sectional view of a single nanoisland. Finally, band-excitation piezoresponse force microscopy (BE-PFM) was used to observe the piezoresponse of individual PTO nanoislands with a commercial AFM system (Asylum Research Cypher) additionally equipped with a Labview/Matlab based controller. The triangle waveform with bias pulses was applied to the samples to induce ferroelectric polarization switching. The changes in the polarization state were measured using BE detection (255–335 kHz) after the application of bias pulses.[22,23]

Results and discussion

Fig. 1 shows SEM and topography images of PTO nanoisland arrays with three different feature sizes. The measured average diameters (d_{NI}) and heights (h_{NI}) of the arrays are given in Table 1. The volume of PTO nanoislands (V_{NI}) was calculated assuming that the nanoislands have a disk-like shape. As seen in Fig. 1 and Table 1, with the decreasing amount of the PTO precursor, the feature size of the PTO nanoislands decreased gradually.

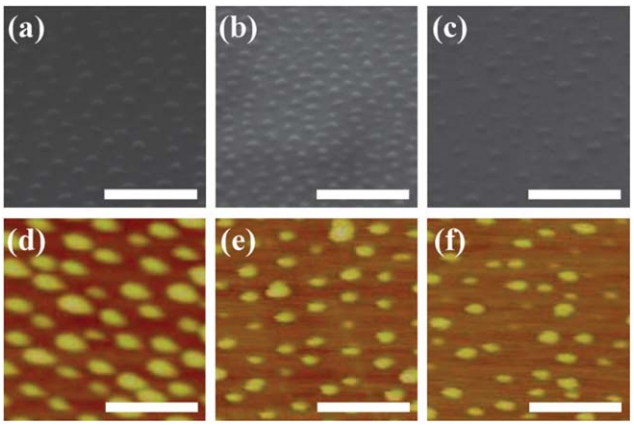

Fig. 1 (top panels) SEM and (bottom panels) topography images of the three different PTO nanoisland arrays. (a and d) The left, (b and e) middle, and (c and f) bottom panels correspond to samples A, B, and C, respectively. Scale bars are 100 nm.

The θ–2θ scan around STO:Nb(001) of sample B shows that PTO(001) is aligned parallel to STO:Nb(001) and no other crystallographic plane is developed [see Fig. 2(a)]. Fig. 2(b) gives mapping in the HL-plane around STO:Nb(001) showing that PTO nanoislands have a c-domain dominant structure. Fig. 2(c) shows the HRTEM image of the cross-sectional view of a PTO nanoisland from sample C. The PTO nanoisland has a disk-like shape with a flattened top surface and steep sidewalls. The width and height were 6.1 nm and 1.5 nm, respectively, which are comparable to the values obtained from the topography in Fig. 1(b). On the other hand, the continuity of the crystal structure between the PTO nanoislands and the substrate confirmed epitaxial relationship between them, which is consistent with XRD data [Fig. 2(a) and (b)]. In the epitaxially grown PTO thin film on a STO(001) substrate, the c-domain usually coexists with the a-domain because of residual stress caused by a mismatch between the film and the substrate.[24,25] However, XRD and HRTEM results revealed that a single PTO nanoisland consists of a single c-domain. Furthermore, it has been reported that crystallographic defects, *e.g.* dislocations and surface dead layers, can invoke instability of spontaneous polarization[26] or pinning of ferroelectric switching.[27] Since crystallographic defects were not found in Fig. 2, the possible effects of these kinds of defects on ferroelectric behavior can be excluded and, therefore, it is expected to show better ferroelectric properties compared to the previously reported ones.

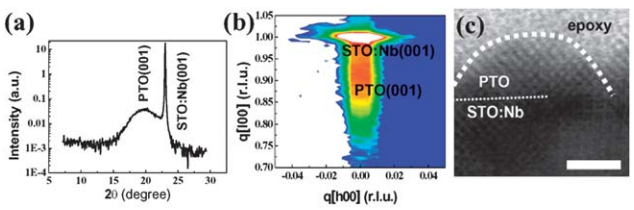

Fig. 2 (a) θ–2θ scan of sample B. (b) Reciprocal lattice space mapping around STO(001) in the HL-plane. (c) Cross-sectional TEM image of sample C. Scale bar is 2 nm.

As shown in Fig. 3, the BE-PFM images show that all the nanoislands have one directional polarization over the scanned area which is consistent with the previously reported results.[15] The existence of spontaneous polarization as well as one directional polarization was also observed in samples B and C (see ESI†). We further examined hysteresis loops of each PTO nanoisland. All the PTO nanoislands, including PTO nanoislands with V_{NI} as small as 79 nm^3 (see Fig. 4), show distinct piezoresponse hysteresis loops suggesting that the polarization can be normally switched by an external electric field. The switchable polarization even for the smallest one can be expected from the absence of crystallographic defects as previously shown in Fig. 2. Furthermore, the contribution of the clamping effect to the piezoelectric coefficient would be negligible because all of the samples lie within the regime of a high scaling ratio (Table 1).[24] On the other hand, the smallest one presents the smallest remnant piezoresponse, which corresponds to the effective piezoelectric coefficient. The decrease of the remnant piezoresponse can be ascribed to the reduction of the number of spontaneous polarizations within a nanoisland. However, samples A and B revealed similar remnant piezoresponse even though the physical dimensions (V_{NI}) are different from each other. This indicates that there can be other factors such as crystal structure and residual stress which can affect the piezoelectric coefficients.

In addition, although the piezoelectric coefficients of the nanoisland arrays were very small compared to the bulk value of PTO (~75 pm V^{-1}), the existence of the switchable polarization was unambiguous. We previously reported that the polarization of PTO nanoislands with V_{NI} of 2660 nm^3 was not switchable.[15]

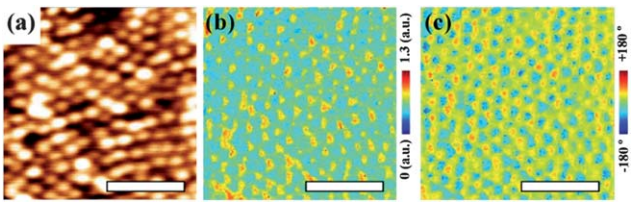

Fig. 3 (a) Topography, (b) BE-PFM amplitude and (c) BE-PFM phase images of the PTO nanoislands in sample A. The BE-PFM images were obtained after topography measurements. Scale bars are 200 nm.

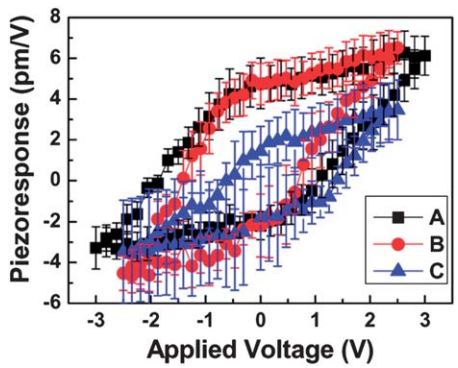

Fig. 4 Piezoresponse hysteresis loops for the nanoislands.

The difference from the previous work can be attributed to the different thermal treatment conditions. In this study, the crystallization was conducted at lower temperature (500 °C) for shorter time (15 min) and at higher cooling/heating rates (1 °C s^{-1}) compared to the previous work (crystallization temperature and time of 600 °C and 1 h respectively, cooling/heating rate of 0.33 °C s^{-1}). It was previously reported that rapid thermal treatments surpass the formation of the undesirable pyrochlore phase, which results in superior properties.[28,29] The improved switching properties might originate from a similar reason. Indeed, when we used the same thermal treatment employed in this study for bigger PTO nanoislands with V_{NI} ~ 2660 nm^3, a distinct hysteresis loop was also observed (see ESI†).

The areal density of the PTO nanoislands with V_{NI} of 79 nm^3 corresponds to ~4.5 Tb in^{-2}. Since the PTO nanoislands with V_{NI} of 79 nm^3 showed switchable polarization, the critical size for ferroelectric nanoislands can be smaller than that. Therefore, there is still room for further increasing the areal density by reducing the interdistance between the individual nanoislands. If the center-to-center distance of the nanoislands can be reduced to 8.5 nm, an areal density of over 10 Tb in^{-2} can be achieved. For instance, employing the so-called 'crew-cut' micelles,[30] the corona of which is much shorter than the core, can allow fabrication of nanostructures with decreased center-to-center distance of the nanoislands, while maintaining the feature size.

Conclusions

In summary, we fabricated uniformly distributed switchable sub-10 nm PTO nanoislands by utilizing block copolymer micelles. The PTO nanoislands were grown epitaxially on a single crystalline substrate without any dislocation at the interface and surface defect. Distinct piezoresponse with switchable polarization was observed even for the PTO nanoislands with a volume of 79 nm^3 (sub-10 nm regime). The results suggest that the critical size of ferroelectrics could be further downsized and, therefore, the areal density of the ferroelectric memory devices would be increased.

Acknowledgements

This research was supported by the National Creative Research Initiative Program supported by the National Research Foundation of Korea (NRF) and a grant (Code no. 2011-0031635) from the Center for Advanced Soft Electronics under the Global Frontier Research Program of the Ministry of Science, ICT & Future Planning, Korea. The research was also supported (S.V.K., Y.K.) by the U.S. Department of Energy, Basic Energy Sciences, Materials Sciences and Engineering Division. A portion of this research was conducted at the Center for Nanophase Materials Sciences (S.V.K.), which is sponsored at Oak Ridge National Laboratory by the Scientific User Facilities Division, Office of Basic Energy Sciences, U.S. Department of Energy. XRD experiments were performed at PLS beamlines 3C2 and 10C1 supported by POSCO and NRF.

Notes and references

1 A. Gruverman, O. Auciello and H. Tokumoto, *Annu. Rev. Mater. Sci.*, 1998, **28**, 101.
2 Y. Cho, S. Hashimoto, N. Odagawa, K. Tanaka and Y. Hiranaga, *Nanotechnology*, 2006, **17**(7), S137.
3 C. H. Ahn, K. M. Rabe and J.-M. Triscone, *Science*, 2004, **303**(5657), 488.
4 C. S. Ganpule, A. Stanishevsky, Q. Su, S. Aggarwal, J. Melngailis, E. Williams and R. Ramesh, *Appl. Phys. Lett.*, 1999, **75**(3), 409.
5 H. Han, Y. Kim, M. Alexe, D. Hesse and W. Lee, *Adv. Mater.*, 2011, **23**(40), 4599.
6 D. D. Fong, G. B. Stephenson, S. K. Streiffer, J. A. Eastman, O. Auciello, P. H. Fuoss and C. Thompson, *Science*, 2004, **304**, 1650.
7 A. Roelofs, T. Schneller, K. Szot and R. Waser, *Nanotechnology*, 2003, **14**(2), 250.
8 H. Fujisawa, M. Okaniwa, H. Nonomura, M. Shimizu and H. Niu, *J. Eur. Ceram. Soc.*, 2004, **24**, 1641.
9 I. Szafraniak, C. Harnagea, R. Scholz, S. Bhattacharyya, D. Hesse and M. Alexe, *Appl. Phys. Lett.*, 2003, **83**(11), 2211.
10 W. Lee, H. Han, A. Lotnyk, M. A. Schubert, S. Senz, M. Alexe, D. Hesse, S. Baik and U. Gösele, *Nat. Nanotechnol.*, 2008, **3**, 402.
11 J. Y. Son, Y.-H. Shin, S. Ryu, H. Kim and H. M. Jang, *J. Am. Chem. Soc.*, 2009, **131**(41), 14676.
12 K. Ishikawa, K. Yoshikawa and N. Okada, *Phys. Rev. B: Condens. Matter Mater. Phys.*, 1988, **37**(10), 5852.
13 B. Su, T. W. Button and C. B. Ponton, *J. Mater. Sci.*, 2004, **39**, 6439.
14 B. Jiang, J. L. Peng, L. A. Bursill and W. L. Zhong, *J. Appl. Phys.*, 2000, **87**(7), 3462.
15 Y. Kim, H. Han, Y. Kim, W. Lee, M. Alexe, S. Baik and J. K. Kim, *Nano Lett.*, 2010, **10**(6), 2141.
16 S. Förster and M. Antonietti, *Adv. Mater.*, 1998, **10**(3), 195.
17 S.-H. Yun, S. I. Yoo, J. C. Jung, W.-C. Zin and B.-H. Sohn, *Chem. Mater.*, 2006, **18**, 5646.
18 S. P. Antony and J. K. Kim, *Chem. Commun.*, 2008, 1193.
19 S. P. Anthony, W. J. Cho, J. I. Lee and J. K. Kim, *J. Mater. Chem.*, 2009, **19**, 280.
20 J. K. Kim, S. Y. Yang, Y. Lee and Y. Kim, *Prog. Polym. Sci.*, 2010, **35**, 1325.
21 S. Kim, S. W. Heo, H. J. Kim, T. Chang, S. B. Kim and J. K. Kim, *Soft Matter*, 2013, **9**, 5550.
22 E. Strelcov, Y. Kim, J. C. Uang, Y. H. Chu, P. Yu, X. Lu, S. Jesse and S. V. Kalinin, *Appl. Phys. Lett.*, 2012, **101**, 192902.
23 Y. Kim, A. Kumar, O. Ovchinnikov, S. Jesse, H. Han, D. Pantel, I. Vrejoiu, W. Lee, D. Hesse, M. Alexe and S. V. Kalinin, *ACS Nano*, 2012, **6**, 491.
24 K. Lee and S. Baik, *Annu. Rev. Mater. Sci.*, 2006, **36**, 81.
25 C. D. Theis and D. G. Schlom, *J. Mater. Res.*, 1997, **12**(5), 1297.
26 M.-W. Chu, I. Szafraniak, R. Scholz, C. Harnagea, D. Hesse, M. Alexe and U. Gösele, *Nat. Mater.*, 2004, **3**, 87.
27 M. Alexe, C. Harnagea, D. Hesse and U. Gösele, *Appl. Phys. Lett.*, 2001, **79**(2), 242.
28 H. Hu, C. J. Peng and S. B. Krupanidhi, *Thin Solid Films*, 1993, **223**(2), 327.
29 D. Szwarcman, D. Vestler and G. Markovich, *ACS Nano*, 2011, **5**(1), 507.
30 W. J. Cho, Y. Kim and J. K. Kim, *ACS Nano*, 2012, **6**(1), 249.

